

Nilo A. Avila, MD
Clara C. Chen, MD
Shan C. Chu, MD
Margaret Wu, PhD
Elizabeth C. Jones, MD
Ronald D. Neumann, MD
Joel Moss, MD, PhD

Index terms:

Computed tomography (CT), comparative studies, 60.1211, 60.12118

Computed tomography (CT), thin-section, 60.12118

Lung, CT, 60.1211, 60.12118

Lung, cysts, 60.312

Lung, diseases, 60.3159, 94.829

Lymphangiomyomatosis, 60.3159, 94.829

Radiography, comparative studies, 60.11

Radionuclide imaging, comparative studies, 60.12171, 60.12176

Radiology 2000; 214:441-446

Abbreviations:

D_{lco} = diffusing capacity of lung for carbon monoxide

DTPA = diethylenetriaminepentaacetic acid

FEV₁ = forced expiratory volume in one second

FVC = forced vital capacity

TLC = total lung capacity

V-P = ventilation-perfusion

¹ From the Departments of Diagnostic Radiology, Warren Grant Magnuson Clinical Center (N.A.A., E.C.J.) and Nuclear Medicine (C.C.C., R.D.N.), the Pulmonary-Critical Care Medicine Branch (S.C.C., J.M.), and the Office of Biostatistics Research, Division of Epidemiology and Clinical Applications (M.W.), National Heart, Lung, and Blood Institute, National Institutes of Health, Bldg 10, Rm 1C-660, 10 Center Dr, MSC 1182, Bethesda, MD 20892-1182. From the 1998 RSNA scientific assembly. Received December 9, 1998; revision requested December 30; final revision received May 20, 1999; accepted June 7. **Address reprint requests to** N.A.A. (e-mail: navila@nih.gov).

© RSNA, 2000

Author contributions:

Guarantor of integrity of entire study, N.A.A.; study concepts, N.A.A., C.C.C., J.M.; study design, N.A.A., C.C.C., S.C.C.; definition of intellectual content, N.A.A., C.C.C.; literature research, N.A.A., C.C.C.; clinical studies, N.A.A., C.C.C., S.C.C., J.M.; data acquisition, N.A.A., C.C.C., S.C.C., E.C.J., R.D.N.; data analysis, N.A.A., C.C.C., M.W.; statistical analysis, M.W.; manuscript preparation, N.A.A., C.C.C.; manuscript editing and review, all authors

Pulmonary Lymphangiomyomatosis: Correlation of Ventilation-Perfusion Scintigraphy, Chest Radiography, and CT with Pulmonary Function Tests¹

PURPOSE: To determine the findings on ventilation-perfusion (V-P) scintigrams, computed tomographic (CT) scans, and chest radiographs and correlate them with pulmonary function test results in patients with lymphangiomyomatosis.

MATERIALS AND METHODS: V-P scintigraphy, chest radiography, conventional and thin-section CT, and pulmonary function tests were performed in 39 patients. The images were graded on a scale of 0 (normal) to 3 (severely abnormal).

RESULTS: Imaging abnormalities were found on 92% of ventilation scintigrams, 92% of perfusion scintigrams, 79% of chest radiographs, 100% of CT scans, and 100% of thin-section CT scans. On ventilation scintigrams, 28 (72%) patients demonstrated a speckling pattern. On CT scans, all patients had pulmonary cysts. Univariate analysis showed that extent of disease on chest radiographs and CT scans, cyst size, V-P abnormalities, and degree of speckling were inversely correlated with forced expiratory volume in one second (FEV₁), diffusing capacity of lung for carbon monoxide, and the ratio of FEV₁ to forced vital capacity (FVC) ($P < .01$) but not with FVC and total lung capacity. Larger cyst size correlated with extent of disease at CT, but not significantly ($P = .056$).

CONCLUSION: Scintigraphic and radiologic abnormalities are seen in a majority of patients with lymphangiomyomatosis. On ventilation scintigrams, a frequently seen speckling pattern may be related to accumulation of radionuclide in pulmonary cysts—a hallmark of the disease at CT. Findings with each imaging modality correlate with certain pulmonary functions.

Lymphangiomyomatosis is a rare, idiopathic disease affecting exclusively women and is characterized by progressive smooth muscle proliferation in the pulmonary lymphatic vessels, blood vessels, and airways (1). The classic chest radiographic manifestations include interstitial pulmonary disease, recurrent pneumothoraces, and chylous pleural effusions (2). The interstitial changes shown on radiographs actually result from superimposition of parenchymal cysts, which are a hallmark of this disease and which are best demonstrated at computed tomography (CT) (3-9).

The purpose of this study was to determine the findings on ventilation-perfusion (V-P) scintigrams, chest radiographs, and CT scans and to compare them with the results of pulmonary function tests in a large group of patients with lymphangiomyomatosis.

MATERIALS AND METHODS

The study protocol was approved by the institutional review board at the National Heart, Lung, and Blood Institute. Subjects were informed of the risks and the benefits of the study.

Written informed consent was obtained from all study participants.

We examined 39 women (age range, 23–54 years; mean age \pm SD, 42 years \pm 9) with a previously established diagnosis of lymphangiomyomatosis and without evidence of tuberous sclerosis. The mean duration between the diagnosis of disease and the time of our evaluation was 4.0 years \pm 3.5 (range, 1 month to 15.5 years). The diagnosis of pulmonary lymphangiomyomatosis was established by means of open pulmonary biopsy (17 patients), thoracoscopic pulmonary biopsy (10 patients), transbronchial biopsy (four patients), and retroperitoneal lymph node biopsy (three patients).

Five patients did not have a pulmonary tissue diagnosis of lymphangiomyomatosis. These five patients had classic clinical and imaging findings at chest CT, which consisted of diffusely scattered thin-walled pulmonary cysts. Of these five patients, three had a history of pneumothorax and renal angiomyolipoma diagnosed after total nephrectomy, one had persistent chylothorax and a history of hemoptysis and recurrent pneumothoraces, and one had a history of recurrent pneumothoraces and transbronchial biopsy results that were consistent with, but not diagnostic of, lymphangiomyomatosis.

Each patient underwent the following studies: aerosol V-P scintigraphy, anteroposterior and lateral chest radiography, conventional CT, thin-section CT, and pulmonary function tests. These studies were performed within 5 days of each other in all patients. Imaging studies were interpreted by board-certified radiologists and nuclear medicine physicians who were aware of the patients' diagnosis but blinded to their clinical status or the results of other imaging modalities or pulmonary function tests. In the first 31 patients, each study was read independently by two radiologists (N.A.A., E.C.J.) or by two nuclear medicine physicians (C.C.C., R.D.N.) to determine interobserver variability. For the correlative analysis performed in all 39 patients, studies were scored by a single radiologist (N.A.A.) or nuclear medicine physician (C.C.C.) who used the methods outlined in this article.

Chest Radiography

Chest radiographs were evaluated for the presence and severity of underlying disease in each of three equal pulmonary zones from apex to base. Abnormalities were characterized as cysts, reticulation,

TABLE 1
Grade Distribution of Imaging Studies

Imaging Modality	Grade			
	0	1	2	3
Radiography overall extent	8 (21)	15 (38)	8 (21)	8 (21)
CT				
Average cyst size	0	11 (28)	20 (51)	8 (21)
Overall extent	0	10 (26)	15 (38)	14 (36)
V-P scintigraphy				
Ventilation*	3 (8)	19 (50)	8 (21)	8 (21)
Perfusion	3 (8)	15 (38)	14 (36)	7 (18)
Speckling	11 (28)	11 (28)	12 (31)	5 (13)

Note.—Data are the number of patients ($n = 39$). Data in parentheses are percentages.

* One ventilation study was uninterpretable for technical reasons.

pleural thickening, and/or pleural effusion. Cysts were defined as areas of decreased opacity with visible walls. Reticulation was defined as a network of straight or curved lines without associated central lucencies. The severity of abnormalities was graded on a four-point scale for each zone as follows: 0, absent; 1, mild; 2, moderate; 3, severe. For each patient, these grades were averaged across all pulmonary zones to provide a global score for the overall severity of involvement of the pulmonary parenchyma.

CT Scanning

CT scanning (HiSpeed Advantage; GE Medical Systems, Milwaukee, Wis) of the chest was performed in all patients. The scans were obtained with 10.0-mm collimation at 1-cm intervals. In addition, thin-section scans with 1.0-mm collimation were obtained at 3-cm intervals. As with the radiographs, the extent of involvement of each of three equal pulmonary zones was assessed independently and graded according to the percentage of the volume judged abnormal as follows: 0, absent; 1, less than 30% abnormal; 2, 30%–60% abnormal; 3, more than 60% abnormal. A mean, global score was also obtained. Pulmonary cysts were evaluated by using thin-section CT to determine the predominant or mean cyst diameter as follows: 1, less than 0.5 cm; 2, 0.5–1.0 cm; 3, more than 1.0 cm. Furthermore, abnormalities were assessed for symmetry and distribution.

V-P Scintigraphy

Aerosol V-P pulmonary scintigraphy was performed in all patients by using a low-energy all-purpose parallel-hole collimator and a gamma camera (Orbitor; Siemens Medical Systems, Hoffman Es-

tates, Ill) peaked to 140 keV with a 20% window. Technetium 99m diethylenetriaminepentaacetic acid (DTPA; Techneplex; Bracco Diagnostics, Princeton, NJ) aerosol ventilation studies were performed by using nebulizers (Aerovent; Medi Nuclear, Baldwin Park, Calif). Patients were placed in a seated position, the DTPA aerosol was administered until a count rate of approximately 2,000 counts per second was achieved, and images of the lungs were obtained in multiple projections. After this, 5–6 mCi (185–222 MBq) of ^{99m}Tc macroaggregated albumin (Pulmolite; Dupont Pharmaceuticals, Billerica, Mass) was administered intravenously, and imaging was repeated.

V-P scintigrams were evaluated qualitatively for abnormalities in ventilation and perfusion by using the following scale: 0, absent; 1, mild; 2, moderate; 3, severe. In addition, ventilation studies were scored for the degree of speckling seen, as distinguished from clumping of aerosol in the large airways. This speckling pattern has been reported before in lymphangiomyomatosis and appears distinct from the usual appearance of central clumping (10). Mean, global scores were obtained for ventilation, perfusion, and speckling.

Pulmonary Function Studies

Spirometry and measurement of functional residual capacity and diffusing capacity of lung for carbon monoxide (DLCO) were performed with the patients in a seated position and with use of a computerized system (Gold Standard PLUS; Warren E. Collins, Braintree, Mass). Spirometry and DLCO measurements were obtained by using standard techniques recommended by the American Thoracic Society (11,12). Functional residual capacity was measured by using the closed-

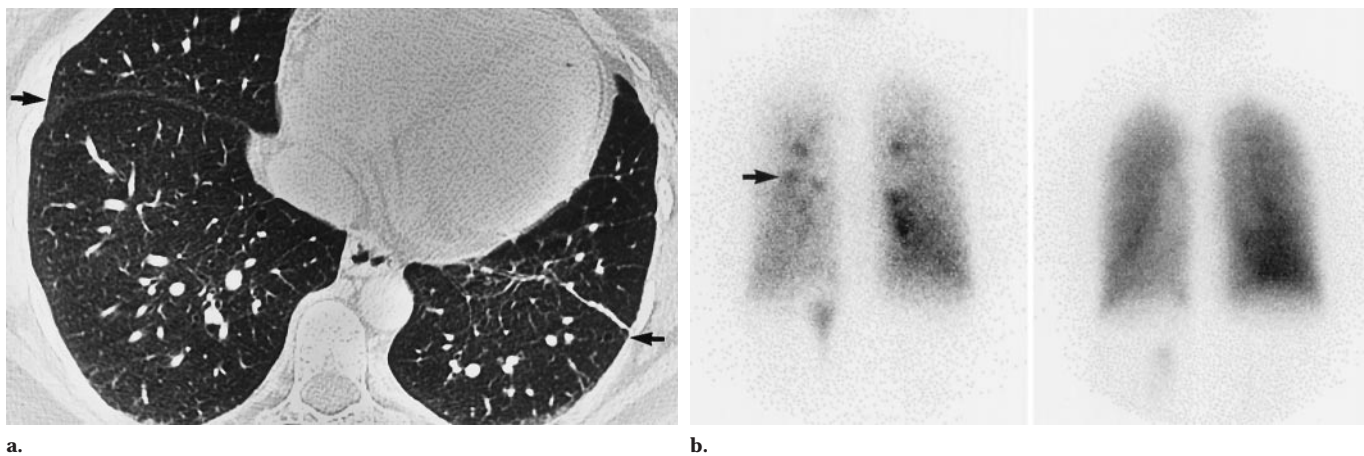


Figure 1. Lymphangioleiomyomatosis in a 35-year-old woman. (a) Transverse thin-section CT scan and (b) posterior ventilation (left) and perfusion (right) images demonstrate minimal extent of disease visible on the CT scan, which consists of pulmonary cysts (arrows in a) involving less than 30% of the lungs, normal ventilation, minimally abnormal perfusion, and minimal speckling (arrow in b).

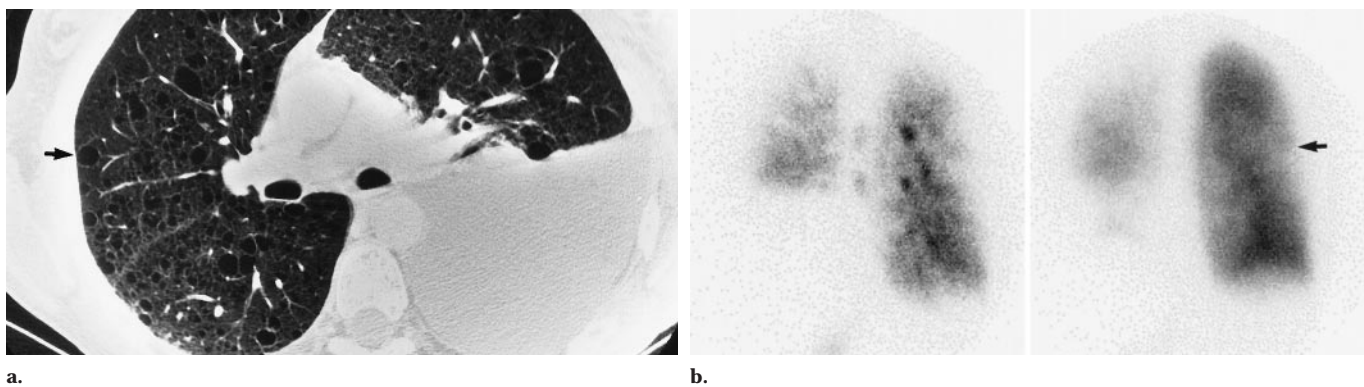


Figure 2. Lymphangioleiomyomatosis in a 54-year-old woman. (a) Transverse thin-section CT scan and (b) posterior ventilation (left) and perfusion (right) images show the moderate extent of disease visible on the CT scan, which consists of pulmonary cysts (arrow in a) involving 30%–60% of the lungs; mild ventilatory abnormalities, aside from the defect caused by pleural effusion; moderate perfusion defects (arrow in b); and moderate speckling consisting of focal areas of increased uptake of radionuclide in the lungs.

circuit helium equilibration technique, with equilibration time of 3–10 minutes. The expiratory reserve volume was subtracted from the functional residual capacity to obtain the residual volume, and the vital volume capacity was added to the residual volume to obtain the total lung capacity (TLC). The predicted values for all pulmonary functions were derived from published standards (13–15).

Statistical Methods

The κ statistic for observer agreement of the imaging studies was calculated according to standard methods for proportions: poor, $\kappa = 0$ –0.39; fair to good, $\kappa = 0.40$ –0.75; excellent, $\kappa = 0.76$ –1.00 (16). Spearman rank correlation coefficients were calculated between the pulmonary function measurements and the global scores on the various imaging studies.

The significance probabilities, or P values, for these correlation coefficients were derived from the t distribution (17,18). A P value less than .05 was considered to indicate a statistically significant difference. Statistical analyses were performed by using a statistical package (SAS; SAS Institute, Cary, NC) (18).

RESULTS

Interobserver Variability

For the purpose of evaluating reader agreement, the imaging studies of the first 31 patients were read independently by two readers. Based on rating scales of four grade levels (0–3), the κ statistics between readers were 0.78, 0.85, and 0.72 for overall chest radiograph grade, overall CT grade, and predominant cyst size grade, respectively. The κ statistics for

ventilation, perfusion, and speckling were 0.48, 0.62, and 0.43, respectively.

Radiologic Findings

Chest radiography.—Eight (21%) of 39 patients had normal chest radiographs (grade 0); the remaining 79% had increased reticular markings (Table 1). Overall extent of disease on chest radiographs was graded as follows: grade 1, 15 (38%) of 39 patients; grade 2, eight (21%) patients; and grade 3, eight (21%) patients (Table 1). Less common findings on radiographs included pleural effusions in five (13%) patients and pneumothoraces in two (5%). Only three (8%) patients had clearly defined cysts on chest radiographs.

Chest CT.—Pulmonary cysts were seen on CT scans in all patients. Cyst walls varied in thickness from faintly percep-

tible to 2.0 mm; the majority were less than 2.0 mm in thickness. Some cysts had no discernable walls and were indistinguishable from emphysema. The extent of pulmonary involvement with cysts was as follows: grade 1, 10 (26%) of 39 patients; grade 2, 15 (38%) patients; and grade 3, 14 (36%) patients (Table 1) (Figs 1–3). Thirty-six (92%) of 39 patients had pulmonary cysts on CT scans that were not apparent on radiographs.

Thin-section CT qualitatively demonstrated the parenchymal cysts better than conventional CT and showed no evidence of interstitial pulmonary disease such as thickening of the interlobular septae in any of the patients. Regarding the predominant cyst size, 11 (28%) of 39 patients had cysts predominantly smaller than 0.5 cm (grade 1), 20 (51%) had cysts predominantly between 0.5 and 1.0 cm (grade 2), and eight (21%) had cysts that were predominantly greater than 1.0 cm (grade 3) (Table 1). Although there was a correlation between the predominant cyst size and disease extent on CT scans, it was not statistically significant ($P = .056$). Patients with the greatest extent of disease did not necessarily have the largest cysts. In two of 10 patients with disease involving less than one-third of the pulmonary parenchyma on CT scans (grade 1), the predominant cyst size was greater than 1.0 cm in diameter (grade 3). On the other hand, in one of 14 patients with disease involving more than two-thirds of the pulmonary parenchyma (grade 3), the predominant cyst size was less than 0.5 cm in diameter (grade 1).

Other less common findings at CT included pneumothorax in two (5%) of 39 patients, pericardial effusion in two (5%) patients, dilated thoracic duct in six (15%) patients, pleural effusions in six (15%) patients, precarinal lymph nodes in two (5%) patients, and retrocrural lymph nodes in two (5%) patients.

V-P scintigraphy.—One patient had a study that was uninterpretable with respect to ventilation abnormalities owing to marked central clumping. Of the remaining 38 studies, ventilatory abnormalities were judged to be absent (grade 0) in three (8%) patients, grade 1 in 19 (50%), grade 2 in eight (21%), and grade 3 in eight (21%). Of the 39 perfusion scintigrams, three (8%) were normal (grade 0), 15 (38%) were grade 1, 14 (36%) were grade 2, and seven (18%) were grade 3. In general, the location of ventilation and perfusion abnormalities matched. In some cases, however, the severity of the decrease in ventilation may have been more or less than the severity of the decrease in

perfusion in the same area. Speckling was seen in 28 (72%) of 39 patients: mild (grade 1) in 11 (28%), moderate (grade 2) in 12 (31%), and marked (grade 3) in five (13%) (Table 1) (Figs 1–3).

Pulmonary function studies.—The results of the pulmonary function studies were abnormal in the majority of patients. Overall, forced expiratory volume in one second (FEV_1), the ratio of FEV_1 to forced vital capacity (FVC), and DLCO in the study population were substantially lower than the predicted values. In contrast, the FVC and TLC were similar to the predicted values (Table 2).

Correlation analysis.—Univariate analysis showed that abnormalities of all major imaging parameters (overall ventilation, perfusion, speckling, extent of disease at CT, mean pulmonary cyst size at CT, and chest radiography grades) correlated significantly with impairment of FEV_1 , DLCO, and the ratio of FEV_1 to FVC ($P < .02$) but not with FVC or TLC (Table 3). Ventila-

tion, perfusion, and degree of speckling also correlated with overall chest radiographic results and extent of disease at CT ($P < .05$) (Table 4) and mean cyst size at CT ($P < .001$). Although there was a relationship between increasing cyst size and overall pulmonary involvement at CT ($r = 0.3$), it did not reach statistical significance at the .05 level ($P = .056$).

DISCUSSION

The principal pulmonary finding in patients with lymphangioleiomyomatosis is cysts. These may vary in size from a few millimeters to many centimeters, and they may vary in extent of involvement from a few scattered cysts to diffuse replacement of the lung (3,9,10,19). Some observers think that the cysts develop as a result of air trapping distal to small airways narrowed by smooth muscle proliferation

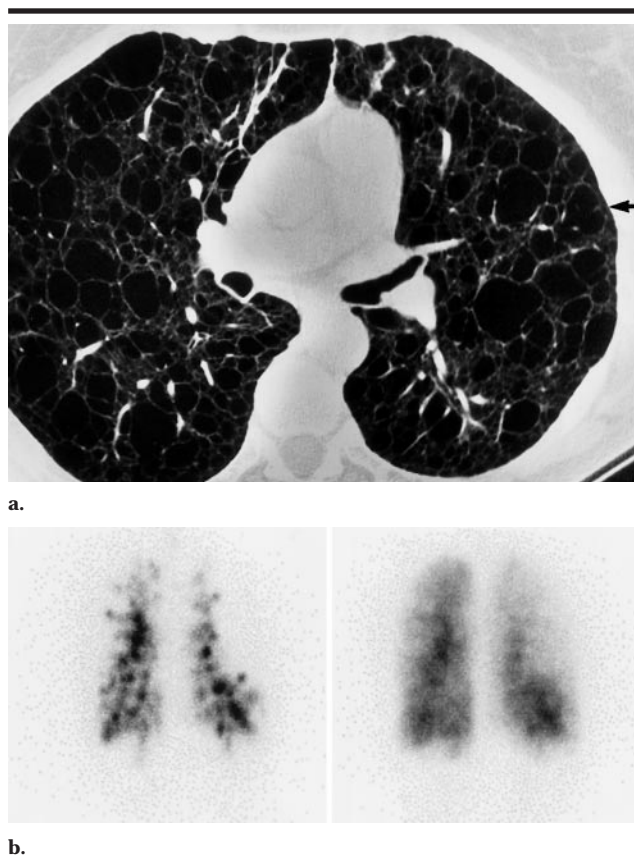


Figure 3. Lymphangioleiomyomatosis in a 52-year-old woman. (a) Transverse thin-section CT scan and (b) posterior ventilation (left) and perfusion (right) images show the severe extent of disease visible on the CT scan, which consists of pulmonary cysts (arrow) involving more than 60% of the lungs, severe ventilation and perfusion abnormalities, and marked speckling consisting of multiple areas of increased uptake of radionuclide that extend to the periphery throughout both lungs.

TABLE 2
Descriptive Data for Percentage of Lung Function Predicted in 39 Patients

Parameter	Mean	SD	Minimum	Maximum
FEV ₁	62.7	25.9	20.0	119.0
FVC	83.9	22.7	34.0	133.0
FEV ₁ /FVC	74.6	22.5	27.0	117.0
TLC	89.1	19.3	54.0	137.0
DLCO	62.4	24.3	19.0	136.0

TABLE 3
Correlation between Imaging and Pulmonary Function Test Results

Imaging Modality	FEV ₁		FVC		FEV ₁ /FVC		TLC		DLCO	
	rValue	PValue	rValue	PValue	rValue	PValue	rValue	PValue	rValue	PValue
Radiography overall extent	-0.43	.006	-0.14	.406	-0.46	.004	0.01	.965	-0.75	<.001
CT Average cyst size	-0.50	.001	-0.19	.246	-0.49	.002	0.03	.867	-0.56	<.001
CT Overall extent	-0.38	.017	-0.14	.396	-0.46	.003	0.02	.925	-0.64	<.001
V-P scintigraphy Ventilation	-0.69	<.001	-0.24	.143	-0.69	<.001	0.06	.727	-0.63	<.001
V-P scintigraphy Perfusion	-0.78	<.001	-0.25	.130	-0.83	<.001	0.06	.730	-0.71	<.001
V-P scintigraphy Speckling	-0.62	<.001	-0.20	.221	-0.72	<.001	0.09	.601	-0.55	<.001

TABLE 4
Correlation between Radiologic and Scintigraphic Findings

V-P Scintigraphy	Radiography Overall Extent		CT Average Cyst Size*		CT Overall Extent	
	rValue	PValue	rValue	PValue	rValue	PValue
Ventilation	0.56	<.001	0.60	<.001	0.40	.014
Perfusion	0.58	<.001	0.64	<.001	0.53	<.001
Speckling	0.46	.003	0.58	<.001	0.33	.038

* The correlation between average CT cyst size and overall lung involvement at CT was $r = 0.30$ with $P = .064$.

(2,19). Others have shown lymphangioleiomyomatosis cells producing matrix metalloproteinases that destroy both collagen and elastin in the pulmonary interstitium. This suggests a role for these enzymes and the breakdown of pulmonary parenchyma in the pathogenesis of the cysts (20).

Evaluation of the pulmonary cysts in lymphangioleiomyomatosis is best done with CT; chest radiographs often fail to demonstrate or may lead to underestimation of the extent of disease. As reported by others (3,4,8,9,21), we found substantial discrepancies between the radiographic and CT findings in many of the patients in our study. In our series, 36 (92%) of 39 patients had pulmonary cysts on CT scans that were not apparent on radiographs. In most of these patients, only nonspecific irregular linear opacities suggestive of interstitial disease were seen on chest radiographs. Only when the

cysts were greater than 1.0 cm in diameter were they recognized on chest radiographs.

Results of previous studies (8,9) led to similar conclusions. The reticular interstitial pattern shown on chest radiographs in patients with lymphangioleiomyomatosis results from summation of numerous cyst walls. Overall, CT affords a more reliable depiction of pulmonary interstitial morphology by virtue of superior contrast resolution and, with thin-section techniques, reduced superimposition or volume averaging effects (22,23).

Fanti et al (10) described a pattern of "well-defined hot spots" on a Technegas ventilation scintigram in a single patient with lymphangioleiomyomatosis, and they postulated this pattern represented accumulation of radionuclide in peripheral cysts. Aerosol DTPA droplets, which adhere to the cyst walls, presumably coalesce and result in focal collections of

activity superimposed on a background of activity within normal alveoli. In this study, we termed this pattern of uptake "speckling" and found the degree of speckling correlated with the extent of disease on CT scans and chest radiographs and with pulmonary dysfunction.

The speckling pattern is nonspecific in its milder forms but has a very distinctive appearance in its severe form, although its actual specificity for lymphangioleiomyomatosis is unknown. For instance, a similar pattern has been described in cystic fibrosis, and it would not be surprising if a similar pattern were seen in other cystic pulmonary diseases such as Langerhans cell histiocytosis (formerly, histiocytosis X) (24). We believe, however, that when severe speckling is present, as seen in 13% of the patients in our study, the pattern strongly suggests the diagnosis of lymphangioleiomyomatosis.

Despite the suggestive appearance of lymphangioleiomyomatosis at CT, the differential diagnosis also includes tuberous sclerosis and Langerhans cell histiocytosis, in addition to emphysema (8,25,26). Identical clinical, radiologic, and histopathologic pulmonary changes may be seen in 1% of patients with tuberous sclerosis (8). Although tuberous sclerosis affects both sexes equally, the pulmonary changes have been described almost exclusively in women (8). Furthermore, tuberous sclerosis, unlike lymphangioleiomyomatosis, is associated with recognized genetic defects. In Langerhans cell histiocytosis, parenchymal cysts are also a primary morphologic feature, although the cyst walls are often more variable in thickness than those seen in lymphangioleiomyomatosis (3,5). In addition, pulmonary nodules and cavitory nodules are a common feature of Langerhans cell histiocytosis (26). Furthermore, Langerhans cell histiocytosis characteristically involves the upper two-thirds of the lungs and spares the costophrenic angles, whereas lymphangioleiomyomatosis involves the lungs diffusely (25,26).

We conclude that lymphangioleiomyomatosis has a characteristic appearance on CT scans and scintigrams, which consists of cysts surrounded by normal lung on CT scans and an abnormal speckling pattern on V-P scintigrams. All major imaging parameters—overall ventilation, perfusion, speckling, extent of disease on CT scans, mean pulmonary cyst size on CT scans, and extent of disease on chest radiographs—correlate significantly with degree of impairment of FEV₁, DLCO, and the ratio of FEV₁ to FVC ($P < .01$) but not with FVC or TLC. The sizes of the pulmo-

nary cysts vary and do not correlate significantly with severity of disease at CT. Larger cyst size, however, correlated significantly with worsening scintigraphic abnormalities, including speckling.

References

1. Corrin B, Liebow AA, Friedman PJ. Pulmonary lymphangiomyomatosis: a review. *Am J Pathol* 1975; 79:348-367.
2. Carrington CB, Cugell DW, Gaensler EA, et al. Lymphangiomyomatosis: physiologic-pathologic-radiologic correlations. *Am Rev Respir Dis* 1977; 116:977-995.
3. Berger JL, Shaff MI. Pulmonary lymphangiomyomatosis. *J Comput Assist Tomogr* 1981; 5:565-567.
4. Merchant RN, Pearson MG, Rankin RN, Morgan WKC. Computerized tomography in the diagnosis of lymphangiomyomatosis. *Am Rev Respir Dis* 1985; 131:295-297.
5. Templeton PA, McCloud TC, Muller NL, Shepard JO, Moore EH. Pulmonary lymphangiomyomatosis: CT and pathologic findings. *J Comput Assist Tomogr* 1989; 13:54-57.
6. Rappaport DC, Weisbrod GL, Herman SJ, Chamberlain DW. Pulmonary lymphangiomyomatosis: high-resolution CT findings in four cases. *AJR Am J Roentgenol* 1989; 152:961-964.
7. Sherrier RH, Chiles C, Roggli V. Pulmonary lymphangiomyomatosis: CT findings. *AJR Am J Roentgenol* 1989; 153:937-940.
8. Müller NL, Chiles C, Kullnig P. Pulmonary lymphangiomyomatosis: correlation of CT with radiographic and functional findings. *Radiology* 1990; 175:335-339.
9. Aberle DR, Hansell DM, Brown K, Tashkin DP. Lymphangiomyomatosis: CT, chest radiographic, and functional correlations. *Radiology* 1990; 176:381-387.
10. Fanti S, Monetti N, Schiavina M, Rimondi MR. Scintigraphic findings in a case of lymphangiomyomatosis. *Clin Nucl Med* 1995; 20:1034-1035.
11. American Thoracic Society. Standardization of spirometry, 1994 update. *Am J Respir Crit Care Med* 1995; 152:1107-1136.
12. American Thoracic Society. Single breath carbon monoxide diffusing capacity (transfer factor): recommendations for a standard technique—1995 update. *Am J Respir Crit Care Med* 1995; 152:2185-2198.
13. Morris JF, Koski A, Johnson LC. Spirometric standards for healthy nonsmoking adults. *Am Rev Respir Dis* 1971; 103:57-67.
14. Goldman HI, Becklake MR. Respiratory function tests: normal values at median altitudes and the prediction of normal results. *Am Rev Tuberc Pulm Dis* 1959; 79:457-467.
15. Gaensler EA, Wright GW. Evaluation of respiratory impairment. *Arch Environ Health* 1966; 12:146-189.
16. Fleiss JL. *Statistical methods for rates and proportions*. 2nd ed. New York, NY: Wiley, 1981.
17. Snedecor GW, Cochran WG. *Statistical methods*. Ames, Iowa: The Iowa State College Press, 1957.
18. *SAS user's guide: basics*. 1982 ed. Cary, NC: SAS Institute, 1982.
19. Braman SS, Mark EJ, McCloud TC, Levine BW. A 32-year-old woman with recurrent pneumothorax: pulmonary lymphangiomyomatosis. *N Engl J Med* 1988; 318:1601-1610.
20. Hayashi T, Fleming MV, Stetler-Stevenson WG, et al. Immunohistochemical study of matrix metalloproteinases (MMPs) and their tissue inhibitors (TIMPs) in pulmonary lymphangiomyomatosis (LAM). *Hum Pathol* 1997; 28:1071-1078.
21. Lenoir S, Grenier P, Brauner MW, et al. Pulmonary lymphangiomyomatosis and tuberous sclerosis: comparison of radiographic and thin-section CT findings. *Radiology* 1990; 175:329-334.
22. Hruban RH, Meziene MA, Zerhouni EA, et al. High resolution computed tomography of inflation-fixed lungs: pathologic-radiologic correlation of centrilobular emphysema. *Am Rev Respir Dis* 1987; 136:935-940.
23. Murata K, Itoh H, Todo G, et al. Centrilobular lesions of the lung: demonstration by high-resolution CT and pathologic correlation. *Radiology* 1986; 161:641-645.
24. Kuni CC, Regelmann WE, duCret PR, et al. Aerosol scintigraphy in the assessment of therapy for cystic fibrosis. *Clin Nucl Med* 1992; 17:90-93.
25. Moore ADA, Godwin JD, Muller NL, et al. Pulmonary histiocytosis X: comparison of radiographic and CT findings. *Radiology* 1989; 172:249-254.
26. Brauner MW, Grenier P, Mouelhi MM, Mompoin D, Lenoir S. Pulmonary histiocytosis X: evaluation with high-resolution CT. *Radiology* 1989; 172:255-258.